Electronic and Magnetic Structure of Cr doped Rutile and Anatase TiO_2; an *ab-initio* DFT+U study.

Winfred M. Mulwa[1]*, Cecil N.M.Ouma[2], Martin O. Onani[3], Francis B. Dejene[1]

[1] Department of Physics, University of the Free State, Qwaqwa Campus, South Africa

[2] Natural Ressources and Environment, CSIR, South Africa

[3]Chemistry Department, University of the Western Cape, South Africa

E-mail: mulwawinfred@gmail.com

Abstract. Semiconductor devices usually utilize the charge of electrons and holes, while magnetic materials used for recording information utilize electron spin. To make use of both charge and spin of electrons in semiconductors, a high concentration of magnetic elements can be introduced in nonmagnetic III-V semiconductors currently in use for devices. The usefulness of semiconductors resides in the ability to dope them with impurities to change their properties, usually to *p*- or *n*-type. This approach can be followed to introduce magnetic elements into nonmagnetic semiconductors to make them magnetic. This category of semiconductors, called diluted magnetic semiconductors, are alloys of nonmagnetic semiconductor and magnetic elements. In our case we investigate chromium-doped TiO_2 in the rutile and anatase phases. We realize that the transition from paramagnetism to ferromagnetism in both phases is at 6% doping. At this point, a large magnetic moment of 2.59 μB and 2.49μB per Cr atom in rutile and anatase respectively was realized.

1. Introduction

TiO_2 plays an important role in the fields of dilute magnetic semiconductors (DMS) and photocatalysis. For both applications TiO_2 requires tailor made electronic properties, which can be manipulated by selectively diluting the system by insertion of dopants. DMS have been investigated in the past in order to gain new insights in the functional principles and the manipulation of the magnetic and semiconducting properties. The search for magnetic semiconductors or for half-metals used for spin-injection led to the discovery of the new material class of d-electron magnets. The prospect of controlling the charge and the electron spin as information carriers would make it possible to combine information processing and storage at the same time [1-3]. The second major application is in the field of photocatalysis, where the favourable electronic gap range of 1.0 to 2.8 eV can be also achieved by doping**.** Impurity doping is an important technique for improving the response of TiO_2-based photoelectrolysis cells [2]. Chromium ions substituted for Ti^{4+} in the TiO_2, lattice have so far yielded optimal results. Substitutional Cr^{3+} in TiO_2 has a strong preference for ferromagnetic ordering. Stabilization of ferromagnetism is achieved through p-type doping. However, the description of the

transition from paramagnetic to ferromagnetic varies within different levels of dopant concentration. We examine the effects of varying Cr^{3+} concentration in the TiO_2 matrix.

In our study, we investigate TiO_2 anatase and rutile doped with chromium atoms, where the Cr is sited at the Ti site at various doping levels. Magnetic order is most common in metallic materials with narrow bands of d electrons therefore in this case, the carriers of the magnetic moments in doped semiconductors TiO_2 is the chromium atoms. The magnetic moment is produced by the d–electrons, this is called d-electron magnetism and has been widely studied in the recent past [4]. Regarding TiO_2 anatase from a photocatalytic aspect, we are mainly interested in the manipulation of the band gap by incorporation of impurities. TiO_2 anatase and rutile phases have band gaps of 3.2 eV [5] and 3.0 eV [6], respectively which corresponds to the ultraviolet region of the absorption spectrum [7]. The creation of electron hole pairs came up due to photon absorption. Photocatalytic and photoelectrochemical applications like the photoinduced decomposition of water on TiO_2 electrodes requires photon absorption as demonstrated by Fujishima and Honda [8]. In the photocatalytic utilization, creation of the electron hole pair makes valence band (VB) become the oxidative band and the conduction band becomes reductive band. Surrounding molecules can therefore be oxidized or reduced for example radicals which are harmful to organic compounds like bacteria and fungi. Therefore, TiO_2 can be used as a purifier removing gaseous or aqueous contaminants [9,10]. In addition to water and air purification, TiO_2 has other photocatalytic applications, like antifogging and self-cleaning surfaces [11]. Since UV light only makes up 5% of the sunlight spectrum we aim to shift the absorption spectrum of TiO_2 into the visible region so as to improve the absorption rate and therefore the photocatalytic efficiency. In this case we modify the band gap using chromium impurities.

2. Calculation details

Within DFT, the electron–electron interaction is expressed as the sum of the Hartree and exchange-correlation (XC) terms although, the XC term is usually approximated. Due to this approximation, the XC term cannot accurately account for electronic interactions in strongly correlated systems, hence the need for DFT+*U* technique where a Hubbard correction *U* is added to the standard DFT formalism 12]. Plane wave method based spin polarized DFT+U calculations were performed as implemented in the Quantum Espresso code [13]. The Perdew-Wang of the local density approximation with the Hubbard U correction (LDA+U) parameterization was utilized for the exchange correlation potentials. The norm-conserving pseudopotentials [14] were used for electron-ion interaction. Doping was performed by substituting one, two, three, four, five, six and seven Ti lattice atoms by Cr atoms corresponding to the Cr doping concentration of 1%, 3%, 4%, 5%, 6%, 8% and 10%, respectively. This was done in order to investigate the effect of doping concentration on the magnetic properties of Cr:TiO_2. A 72 atom supercell was modelled by $2\times 2\times 1$ repetition of the anatase unit cell. Plane waves with an energy up to 60 eV were included in the basis set, in order to avoid Pulay stress and other related problems. The Brillouin-Zone integration was performed using a $2\times 2\times 2$ Γ centered *k*-mesh with Gaussian smearing set to 0.05 eV. The total energy was converged at $1x10^{-6}$ eV. To compare and evaluate the structural changes induced by the impurities, calculations on pure TiO_2 were done initially to obtain structural and electronic data that can be used as a reference. Anatase is computationally stable than rutile and brookite phases therefore we investigated the properties of chromium doped anatase. To investigate the stability of the doped system we calculated the defect formation energies according to the following formula [15].

$$E^{f}[X] = E_{tot}[X] - E_{tot}[bulk] + n(\mu_0 - \mu_x) \quad (1)$$

where E_{tot} is the total energy of the doped supercell with one Ti atom replaced by the impurity *X*(*X*=Cr), E_{tot}[bulk] is the total energy for the pristine system. *n* indicates the number of Ti atoms that have be replaced in the supercell by the dopant atoms, μ_0 and μ_x are the corresponding chemical potentials. The chemical potentials were calculated with respect to the free atom.

In order to get more stable atomic configuration and lattice parameters, the geometry optimization was performed for pure and doped systems using Broyden-Fletcher-Goldfarb-Shanno (BFGS) quasi-newton minimization scheme [16]. Supercells of optimised pure anatase TiO_2 and 6% Cr-doped TiO_2 are shown in figure1.

3. Results and discussions

3.1. Geometrically optimized structure properties

It is only rutile and anatase phases which play a key role in the applications of TiO_2 in industry because of their simple tetragonal structure compared to complicated orthorhombic brookite structure. Many of the technological applications utilize the anatase phase (figure 1) rather than the rutile one, as this appears to be more catalytically active and exhibits a higher electron mobility. Rutile and anatase are both tetragonal, containing 6 and 12 atoms per unit cell, respectively. In both structures each Ti atom is coordinated to six O atoms and each O atom is coordinated to three Ti atoms. In each case, the TiO_6 octahedron is slightly distorted, with two Ti-O bonds slightly greater than the other four, and with some of the O-Ti-O bond angles deviating from 90^o. The distortion is greater in anatase than in rutile. The structure of rutile and anatase crystals has been described frequently in terms of chains of TiO_6 octahedra having common edges [17-18]. Two and four edges are shared in rutile and anatase, respectively.
The calculated lattice parameters after geometry optimization are a = 4.5936Å, c = 2.9587Å and a = 3.784Å, c = 9.515Å for rutile and anatase, respectively from LDA+U calculations. The obtained lattice parameters are in good agreement with other theoretical calculations [19] which implies that our calculation methods are reasonable and the obtained results are trustworthy. The averaged bond lengths of the pure anatase TiO_2 and geometric optimized 0-10% Cr:TiO_2 are provided in table 1. From table 2 the LDA+U obtained lattice parameters confirms what was realized experimentally.
These results also agree very well with Deskins et al findings. [20].

Table 1: Average Mulliken bond lengths of pure and Cr:TiO_2 models after geometry optimization

System	Ti-O(Å)	O-O(Å)	Cr-O(Å)
Pure TiO_2	1.9759	2.719	
1%Cr:TiO_2	1.9445	2.68	1.9353
3%Cr:TiO_2	1.9483	2.678	1.9345
4%Cr:TiO_2	1.9485	2.7001	1.9342
6%Cr:TiO_2	1.9399	2.7101	1.9341
7%Cr:TiO_2	1.9392	2.7111	1.9340
8%Cr:TiO_2	1.9390	2.7111	1.9339
10%Cr:TiO_2	1.9391	2.7112	1.9339

Table 2: A comparison between calculated structural properties of rutile and anatase phases with experimental data.

Rutile	a (Å)	c (Å)
Experiment	4.587[21]	2.954[21]
This work	4.5936	2.9587
Anatase		
Experiment	3.782[21]	9.502[21]
This work	3.784	9.515

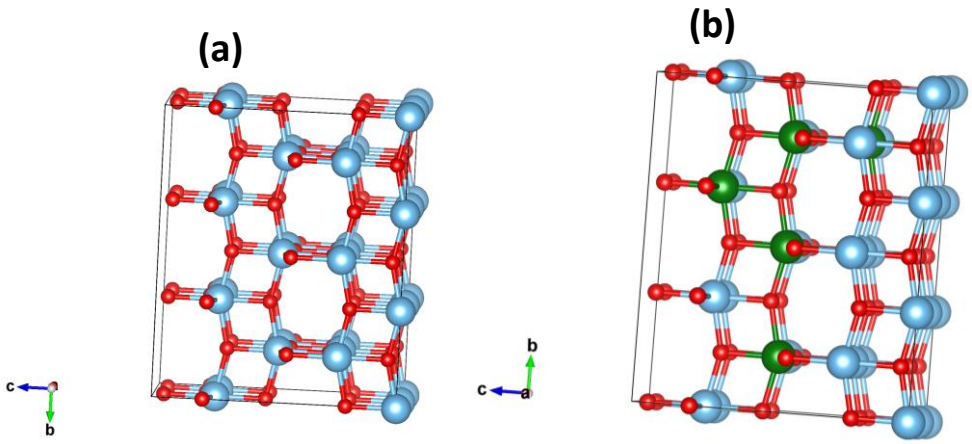

Figure 1: A supercell of a) Pristine TiO_2 b) Cr doped TiO_2 (Red, Blue and Green balls represents O,Ti and dopant atoms respectively).

The geometric optimized structures of pure anatase TiO_2 and 6% Cr-doped anatase were realized by the application of VESTA (Visualization for Electronic and Structural Analysis) [22] visualizing tool as shown in figure 1. In figure 1(a), the blue atoms represent titanium, while the red atoms represent oxygen. In figure 1 (b), the blue atoms are titanium, red atoms are oxygen and green atoms are chromium atoms sited at Ti site. Formation energy was calculated at various substitution sites and sites with the lowest formation energy were utilized.

3.2. Magnetic properties

From the projected density of states output file, at the Lowdin charges part, we were able to get the magnetic moment per Cr atom. A large magnetic moment of 2.59μB in rutile and 2.49μB in anatase per Cr atom is found for 6% Cr-doped rutile and anatase. After 6% doping of TiO_2 with chromium, both phase reached magnetic saturation as shown in figure 2.

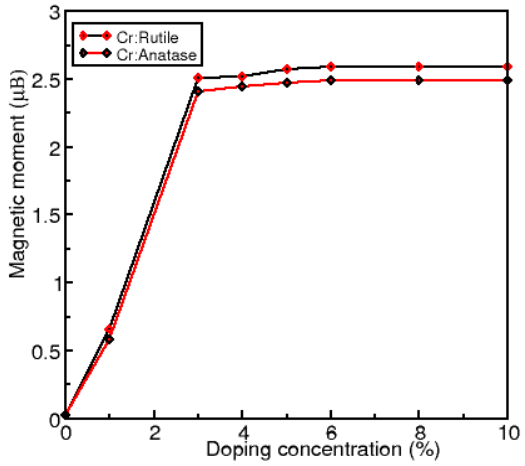

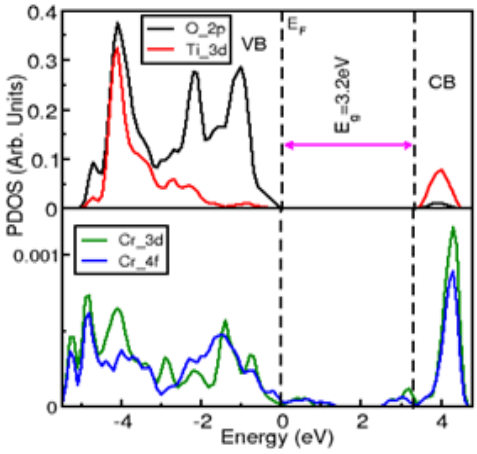

Figure 2: Magnetic saturation in rutile and anatase. **Figure 3:** PDOS of Cr doped TiO_2

The highest magnetic moment of 2.59μB in rutile and 2.49μB in anatase per Cr atom realized in our two phases is higher than expected. Chromium is magnetic, therefore there is a possibility that all the contribution to the magnetic moment is due to Cr ions but there are high chances that Ti moments contributed a certain amount of magnetic moment. When we look at the hybridization of Ti_3d and Cr_3d in figure 3, both Cr and Ti may have contributed to the realized high magnetic moment. The participation of Ti_3d electrons makes the understanding of magnetic properties in rutile and anatase more interesting.

3.3. Electronic properties

The top panel of figure 3 shows pure anatase with a band gap of 3.2 eV which is exactly same as experimental value. This confirms the accuracy of our results. Impurity states are realized just below the conduction band minimum (CBM) as well as above the valence band maximum (VBM), therefore the band gap has been reduced from 3.2 eV to 1 eV after 6% doping of anatase with chromium. Figure 4 (a) and (b) confirm what is realized in figure 3 from density of states point of view.
Figures 3 and 4 show an effective photocatalyst, that is, a band gap with no additional states inside. Additional states inside a band gap become electron-hole traps and recombination centers causing a reduction in the lifetime of the photoinduced charged carries, leading to a decrease of photocatalytic efficiency. Doping our system with chromium, we reduced the band gap in an efficient way, that is without introducing mid band gap states which make the recombination rate of the charge carriers to be maximum. Figure 4 (a) and (b) shows that after 6% doping (part f), the crystal structure undergoes deformation (part g and h). As seen in figure 4 (a) and (b), when the doping percentage is increased, more impurity states appear within the bad gap and the shape of the conduction band and valence band remains the same. After 6% doping (part f), any more increase of Cr in TiO_2 causes a change in the shape of the valence and conduction bands. This is attributed to the crystal structure undergoing deformation (part g and h).

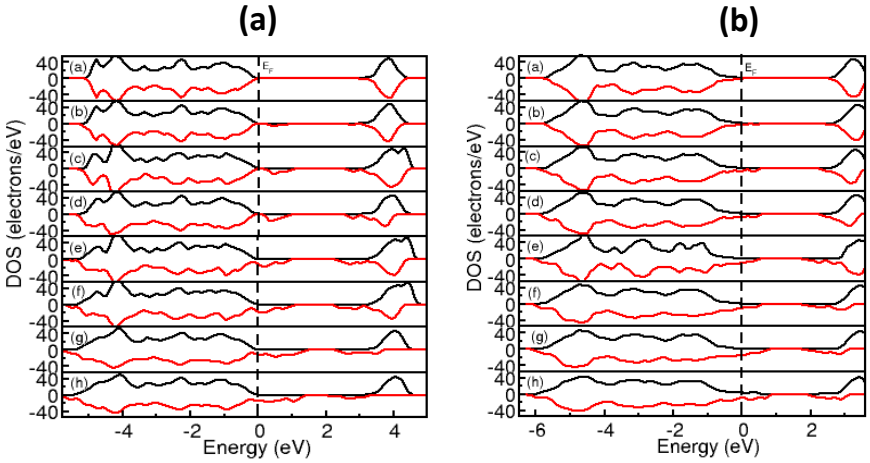

Figure 4: Calculated DOS of pristine and 1-10%Cr:TiO_2 as a function of energy.a) Rutile b) Anatase.

3.4 *Photocatalytic performance.*

The effect of Cr-doping on the photocatalytic effect (clean bandgap) is also shown in figure 4 (a) and (b). As the concentration of Cr is increased, more dopant states are seen to be encroaching into the bandgap both from valence band maximum and conduction band minimum. This represents a shift in the absorption band edge towards longer wavelength with the increasing Cr concentration (red shift).

The red shift is maximum at 4% doping of TiO_2 with Cr which is consistent with the experimental findings [23]. After which the size of the 'clean' band gap remains constant. Even after attaining optimal doping concentration at 4%, with further increase in doping, crystal deformation is achieved at 6% doping, which is also the magnetic saturation point as shown in figure 2.

4. Conclusion

Cr-doped rutile and anatase are magnetic semiconductors. They acquire magnetic moment saturation at 6% doping in each case with 2.59μB in rutile and 2.49μB in anatase. The transition point from paramagnetism to ferromagnetism is at 6% Cr doping in both phases**.** The large magnetic moments originates from two sources, that is, involvement of the 3d electrons of the Cr^{3+} ions and the formation of acceptor bound magnetic polarons, in which the spins of the holes and chromium are aligned through exchange interaction. From figures 3 and 4, we find enhanced photocatalysis because there are no mid band gap states. After 6% magnetic saturation is achieved and addition of more Cr^{3+} atoms does not improve magnetic properties but distorts the crystal lattice. This study clearly shows the importance of doping TiO_2 with Cr to enhance its magnetic and photocatalytic properties.

Acknowledgement

This research work is supported by the national research foundation of South Africa.

References

[1] Ohno H 1998 Science **281** 951.
[2] Matsukura F, Ohno H, Shen A and Sugawara Y 1998 Phys. Rev. B **57** 2037.
[3] DiVincenzo D P 1995 Science **270** 255.
[4] Y.Matsumoto, M.Murakami, T.Shono, T.Hasegawa, T.Fukumura, M.Kawasaki, P.Ahmet, T. Chikyow, S.Koshihara and Koinuma H 2001 Science **291**, 854.
[5] Tang H, Berger H, Schmid P E, Levy F, and Burri G 1993 Solid State Commun. **87**, 847
[6] Pascual J, Camassel J, and Mathieu H 1978 Phys. Rev. B **18**, 5606.
[7] Meng N, Micheal Leung* K H, Dennis Leung Y C, Sumathy K 2007 Renew. Sustainable Energy Rev. **11** 401-425.
[8] Fujishima A and Honda K 1972 Nature **238** 37.
[9] Anne M and Dulay T 1993 Chem. Rev. **93** 341.
[10] Hoffmann M R, Martin S T, Choi W and Bahnemann D W 1995 Chem. Rev. **95** 69.
[11] Lai Y, Tang Y, Gong J, Gong D, Chi L, Lin C and Chen Zc. 2012 J. Mater. Chem.**22** 7420-7426.
[12] Cococcioni M and De Gironcoli S 2005 Phys. Rev. B **71** 35105.
[13] Giannozzi P, Baroni S, Bonini N, Calandra M, Car R, Cavazzoni C, Ceresoli D, Chiarotti G L, M.Cococcioni, I.Dabo, A.Dalcorso, S.Fabris, G.Fratesi, S.deGironcoli F.Mauri, R.Mazzarello, Paolini S, Pasquarello A, Paulatto L, Sbraccia C, Scandolo S, Sclauzero G, Seitsonen A P, Smogunov A, Umari P and Wentzcovitch R M 2009 J.Phys.Condens. Matter **21** 395502.
[14] Hamann D R, Schluter M and Chiang C 1979 Phys. Rev.Lett, **43** 1494-1497.
[15] Van de Walle C G and Neugebauer J 2004 J. Appl. Phy. **95** 385.
[16] Pfrommer B G, Cote M, Loulle S G and Cohen M I 1997 J. Comput. Phys.**131** 233.
[17] Grant F A 1959 Rev. Mod. Phys. **31** 646.
[18] Kavan L, Grtzel M, Gilbert S E, Klemenz C and Scheel H J 1996 J.Am. Chem.Soc. **118** 6716
[19] Arroyo-de Dompablo M E, Morales-Garcia M and Taravillo 2011 J. Chem. Phys. **135** 54503.
[20] Aaron N, Deskins N and Michel D 2007 Phys. Rev. B **75** 195212.
[21] Burdett J K, Hughbanks T, Miller G J, Richardson Jr J W and Smith J V 1987 J.Am. Chem. Soc. **109** 3639.
[22] Momma K and F.Izumi F 2011 J. Appl. Crystallogr. **44** 1272.
[23] Yan-Hua P, Gui-Feng H* and Wei-Qing H* 2012 Adv. Powder Technol. **23** 8-12.